J Polym Res (2015) 22: 35
DOI 10.1007/s10965-014-0591-4

ORIGINAL PAPER

Compatibilization of polypropylene/recycled polyethylene terephthalate blends with maleic anhydride grafted polypropylene in the presence of diallyl phthalate

Yeling Zhu · Changsheng Liang · Yang Bo · Shiai Xu

Received: 25 May 2014 / Accepted: 16 October 2014 / Published online: 11 February 2015
© Springer Science+Business Media Dordrecht 2015

Abstract Bi-functional co-agent, diallyl phthalate (DAP), −assisted melting free-radical grafting of maleic anhydride (MAH) on polypropylene (PP) is carried out by reactive extrusion. The PP/recycled polyethylene terephthalate (rPET) blends with and without PP-g-MAH/DAP (PP grafted with both MAH and DAP) are conducted on a twin-screw extruder. It reveals that the introduction of DAP can significantly enhance the grafting degree of MAH and decrease the chain scission of PP. The maximum extent of MAH grafting (1.5 wt.%) is obtained when DCP and MAH contents are 0.5 and 6.0 wt.%, respectively, and the DAP/MAH molar ratio is 0.3. Besides, differential scanning calorimetry (DSC) analysis shows that the crystallization temperature of grafted PP is higher than that of pure PP due to the nucleation of grafted groups. Fourier transform infrared spectroscopy (FTIR) analysis proves that chemical reactions take place between PP-g-MAH/DAP and rPET. In particular, scanning electron microscopy (SEM) observations demonstrate that, the PP/rPET blends compatibilized with PP-g-MAH/DAP show enhanced adhesion at the interface comparing with the binary PP/rPET blend, which is also proved by DSC measurements, dynamic mechanical analysis (DMA) and mechanical properties.

Keywords Polypropylene · Maleic anhydride · Diallyl phthalate · Recycled polyethylene terephthalate (rPET) · Morphology · Properties

Y. Zhu · C. Liang · Y. Bo · S. Xu (✉)
Shanghai Key Laboratory of Advanced Polymeric Materials, Key Laboratory for Ultrafine Materials of Ministry of Education, School of Materials Science and Engineering, East China University of Science and Technology, Shanghai 200237, China
e-mail: saxu@ecust.edu.cn

S. Xu
The Chemical Engineering College of Qinghai University, Xining 810016, China

Introduction

Polyethylene terephthalate (PET) is an important engineering plastic. One of the main applications for PET is in packaging (bottles, films, containers, etc.), where optical clarity is the main concern [1]. Owing to its broad-scale applications, the need to provide for its post-consumer recycling has become an important challenge in environmental protection and enabling plastics manufacturing technology to be sustainable. During the last decade, many efforts have been directed toward recycling waste PET products [1–13]. Among these, blending PET with PP is very attractive because of its economy and the superior mechanical properties of the blend [6–9].

However, PP and PET are thermodynamically incompatible because of differences in their chemical nature and polarity, their blends therefore tend to separate grossly with weak interfacial bonding and poor mechanical properties [7]. Appropriate compatibilization is necessary to reduce the interfacial tension, achieve good adhesion, and stabilize the domain structure. There are multiple types of compatibilizers applied in PP/PET blends [2, 4, 7, 9, 14–27]. PP grafted with maleic anhydride (PP-g-MAH) is the most common because of its improved polarity and reactivity [14, 24–27]. Now, the reaction of MAH grafted PP in the melting state in the presence of a radical initiator is the most widespread methodology. However, the grafting reaction is generally accompanied by chain scission that results in the reduction of the grafting degree and decrease in the molecular weight.

Much attention has been given to improving the grafting behavior by the introduction of a co-agent. Li et al. [28] and Bettini et al. [29] showed that the presence of the electron-donating monomer styrene (St) in the melting process reduced the PP chain scission and increased the grafting degree of MAH. The maximum extent of MAH was obtained when the MAH/St molar ratio was 1.0. With addition of St, it is likely that MAH and St interact with each other to form a charge transfer

complex (CTC), which leads to a greater extent of grafting and forms a SMA branch on PP. However, St is not a perfect choice because of its high volatility and toxicity. Henry et al. [30, 31] reported that high grafting levels of MAH (2.5 to 3.0 wt.%) were achieved without excessive degradation of the PP chain in a reactive extrusion process by using a brominated co-agent, N-bromosuccinimide (NBS). The bromine radicals are able to reversibly quench PP macroradical, the instantaneous concentration of active free radicals is decreased, promoting grafting instead of chain scission. It must be pointed out that NBS can epimerize the backbone with decrease in the PP-g-MAH crystallinity. Heteroaromatic derivatives have also been used as co-agents during MAH functionalization of PP [32–34]. A co-agent, such as butyl 3-(2-furanyl) propenoate (BFA), which has an electron donating heterocyclic aromatic ring conjugated with a double bond bearing an electron- attracting group substituent, results in a high addition rate to the tertiary polypropylene macroradical with formation of a new resonance-stabilized macroradical that limits the polypropylene degradation and improves the grafting degree. Besides, rare earth oxide has also been used to assist the grafting process [35]. In some cases, poly-functional monomers are recommended. Ni et al. [36] found that use of trimethylol propane triacrylate (TMPTA) as a co-agent improved the grafting degree of MAH and controlled the degradation of the grafted PP. It suggests that TMPTA has high reactivity with both the PP macroradical and MAH, leading to the stabilization of the macroradical, depression of the chain scission and formation of branched PP. Sengupta et al. [37] observed that chain scission in the melting state could be mitigated using the co-agent assisted cross-linking when MAH was grafted with PP. Both triallyl trimesate (TAM) and triallyl phosphate (TAP) were used as co-agents, however, these tri-allylic co-agents had no obvious effect on the grafting degree.

Diallyl phthalate (DAP) is a bi-functional monomer with allylic structure. It is less toxic than St and relatively inexpensive in comparison with tri-functional monomers, such as TMPTA and TAM. To our knowledge, there is no public report on bi-allylic co-agent application in MAH grafted PP. In this work, DAP is used as a co-agent in the grafting process. The effect of DAP on the grafting degree of MAH, melt flow index (MFI) and thermal properties is analyzed. In addition, we study the effectiveness of PP-g-MAH/DAP (PP grafted with both MAH and DAP) as a compatibilizer for PP/recycled PET (rPET) (80/20, *w*/*w*) blends.

Experimental

Materials

PP (K8003) was copolymer grade, supplied by Dushanzi Petrochemical Co., Ltd., with MFI of 2.5 g/10 min (230 °C, 2.16 kg). MAH was commercially available (analytical grade). DAP and the free radical initiator dicumyl peroxide (DCP) were obtained from Aladdin Reagent Co., Ltd., China. rPET was waste bottle grade from Botou Jiaxin Chemical Co., Ltd.

Melt grafting

The PP (100 phr), DCP (0.2 to 1 wt.%), MAH (2 to 10 wt.%), and DAP (the DAP/MAH molar ratios were 0.2, 0.3, 0.5, 0.8, and 1, respectively.) were premixed in a high speed mixer. The grafting reaction was conducted on a co-rotating twin-screw extruder (SHJ-35, Φ =21.7 mm, L/D=32, Nanjing Keya Co., Ltd.). The temperatures of barrels were 170 °C, 190 °C, 195 °C, 190 °C, and 190 °C. The feed screw and the main screw speed were 15 and 30 rpm, respectively.

Blend preparation

The PP/rPET (80/20, *w*/*w*) blends with different amounts of PP-g-MAH/DAP were prepared on a co-rotating twin-screw extruder. The temperatures from the hopper to the die were 200 °C, 250 °C, 255 °C, 250 °C, and 230 °C. The feed screw and the main screw speeds were 30 and 100 rpm, respectively. Before blending, PP, PP-g-MAH/DAP and rPET were dried in a vacuum oven for 12 h at 80 °C, 120 °C and 140 °C, respectively. The resulting products were cut into pellets, dried at 120 °C for 12 h, and then injection molded in an injection-molding machine (JN55-E, Zhenxiong Machinery Factory Co., Ltd.). The procedures for preparing the blends are shown in Fig. 1.

Fourier transform infrared spectroscopy (FTIR) analysis

The grafted PP was Soxhlet-extracted using hot xylene for 24 h to separate out the xylene-insolubles. Excess acetone was then added to the xylene-soluble fraction to give a soluble fraction containing unreacted monomer and co-agent, while the insoluble fraction contained MAH grafted PP. The precipitate was filtered, washed, and then dried in a vacuum oven at 80 °C for 24 h. The purified sample was then hot-pressed into thin films at 190 °C and analyzed by FTIR (Nicolet 5700). The scan number was 32 and the resolution was 4 cm^{-1}.

The possible chemical reaction between PP-g-MAH/DAP and the terminal groups of rPET was also characterized by FTIR. The PP/rPET/(PP-g-MAH/DAP) (80/20/10) blend was Soxhlet-extracted using refluxing trifluoroacetic acid to extract the rPET phase. The insoluble fraction was dried and then hot-pressed into a thin film at 190 °C.

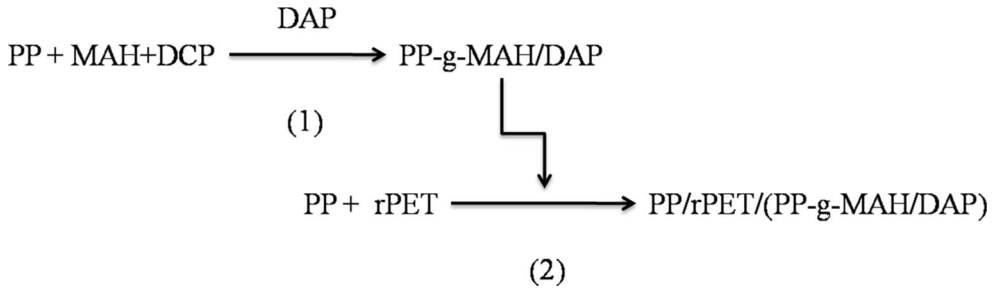

Fig. 1 Procedures for preparing the PP/rPET/(PP-g-MAH/DAP) blends: (1) melt grafting, (2) blend preparation

Determination of the grafting degree of MAH

The grafting degree of MAH was determined by chemical titration. About 0.5 g purified sample was dissolved in 100 mL of refluxing xylene. Then excessive potassium hydroxide (KOH) in ethanol solution was added to the cooled xylene solution, and it was refluxed again for another 1 h. Finally, the hot solution was titrated immediately with hydrochloric acid (HCl) in isopropanol solution with 1 % phenolphthalein as the indicator. The equation used to calculate the acid number (A, mmol KOH/g) is

$$A = (C_1V_1 - C_2V_2)/M \quad (1)$$

where V_1 and V_2 represent the volumes (mL) of KOH solution in ethanol and HCl solution in isopropanol, respectively. C_1 and C_2 were the concentrations (mol/L) of KOH in ethanol solution and HCl in isopropanol solution, respectively, and M (g) is the mass of the purified samples. The grafting degree of MAH (G_{MAH}, wt.%) is calculated as follows,

$$G_{MAH} = 9.806 \times (A - A_0)/2 \quad (2)$$

where A_0 (mmol KOH/g) is the acid number of the purified sample without addition of MAH.

MFI measurement

MFI was performed on a MFI equipment (RSY-1LH-90, Shanghai Liwupu Instrument Co., Ltd.) at 230 °C with a load of 2.16 kg according to the ASTM D1238 standard.

Morphology analysis

The morphologies of the blends were studied by scanning electron microscopy (SEM, S-4800, Hitachi). The samples were fractured in liquid nitrogen, and the fractured surfaces were coated with a thin gold layer before testing. A mixed solvent of phenol/1, 1, 2, 2, tetra chloroethane (60/40, *w*/*w*) was used to extract the rPET phase [16, 38]. The particle size distribution of the dispersed phase was analyzed by measuring the diameter of an appropriate number of particles for each sample by an image analysis program (Nano Measurer 1.2).

Differential scanning calorimetry (DSC) measurement

DSC measurements were conducted on a TA instrument (2910C) used for analysis of thermal properties. The temperature was calibrated with indium. About 8 to 12 mg of grafted PP was accurately weighed. The sample was pre-heated from 25 to 200 °C, held for 2 min, then cooled to 25 °C, and reheated to 200 °C at a constant cooling/heating rate of 10 °C/min. All operations were performed in nitrogen atmosphere.

The uncompatibilized and compatibilized PP/rPET blends were pre-heated from 25 to 280 °C, and held for 2 min, then cooled to 25 °C, and reheated to 280 °C at a constant cooling/heating rate of 10 °C/min.

Dynamic mechanical analysis (DMA)

DMA, conducted on a TA instrument (Q800), was employed to study changes in glass transition temperatures (T_g) of the PP and rPET phases in the uncompatibilized and compatibilized blends. The three-point bending mode was chosen for analysis. The specimens were heated from −50 to 150 °C at a heating rate of 5 °C/min, and the testing was performed at a vibration frequency of 1Hz.

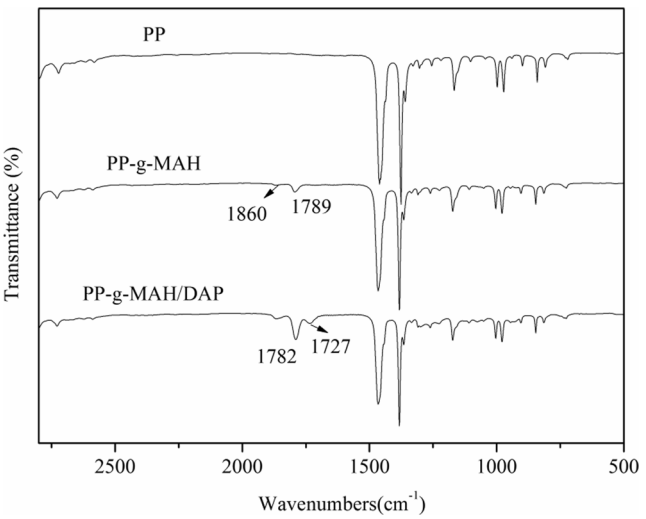

Fig. 2 FTIR spectra of pure PP, and MAH grafted PP without and with DAP

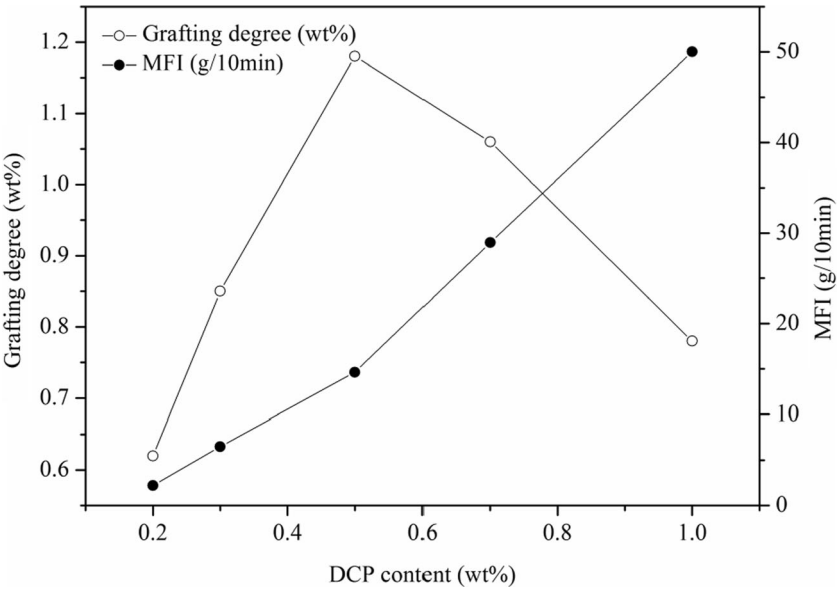

Fig. 3 Effect of DCP content on grafting degree and MFI value (MAH 4.0 wt.%)

Mechanical analysis

Tensile and flexural tests were performed with a SANS universal testing machine (CMT 4204) in accordance with ISO 527 and ISO 178 standards, respectively. The notched impact strength was tested by a Charpy tester (XCJ-4, Chengde Precision Testing Machine Co., Ltd) according to ISO 179 standard.

Results and discussion

Figure 2 displays the FTIR spectra of pure PP, PP-g-MAH (G_{MAH}=0.8 wt.%) and PP-g-MAH/DAP (G_{MAH}=1.5 wt.%). New absorption bands at 1860 cm^{-1} and 1789 cm^{-1} found in PP-g-MAH without DAP, are assigned to the absorption bands of the carbonyl groups (C=O) of MAH. The absorption band at 1727 cm^{-1} observed in PP-g-MAH/DAP, is assigned to C=O of DAP, and the band at 1789 cm^{-1} shifts to 1782 cm^{-1}. De Roover et al. [39] assigned the band at 1790 cm^{-1} to a single succinic anhydride attached to the chain end of PP, and the band at 1782 cm^{-1} was attributed to polymaleic anhydride or other forms of MAH. Bettini et al. [29] suggested that the shift of C=O was due to reaction between St and MAH to form a branch on PP. In the present case, it implies that a change appears in MAH neighboring groups because of the incorporation of DAP.

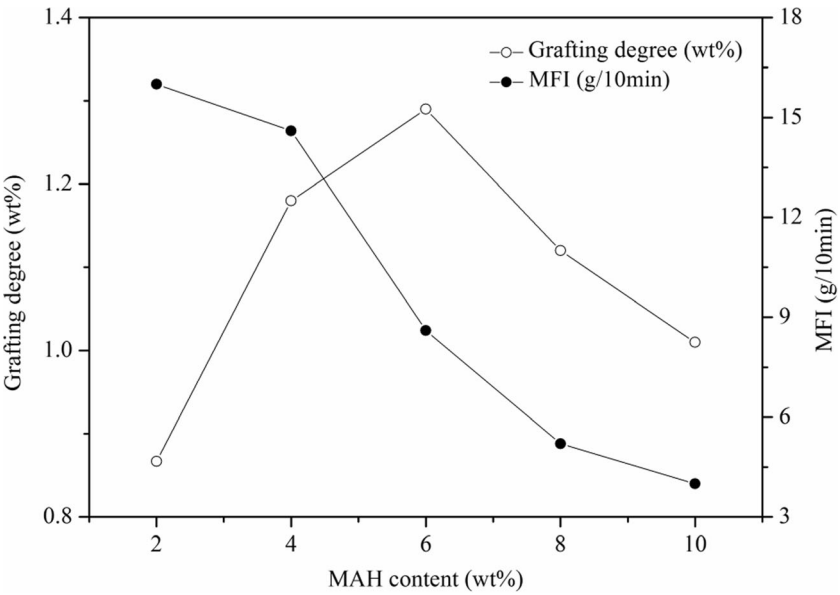

Fig. 4 Effect of MAH content on grafting degree and MFI value (DCP 0.5 wt.%)

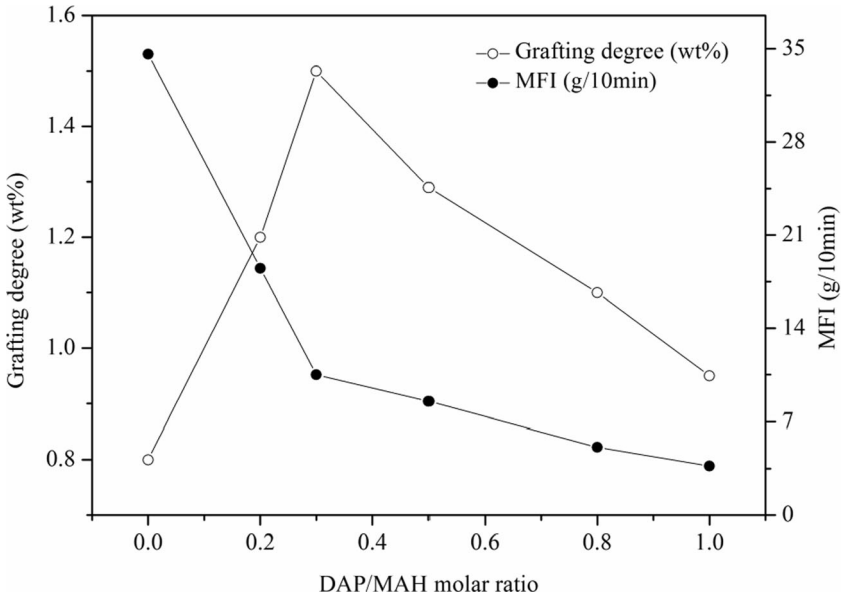

Fig. 5 Effect of DAP/MAH molar ratio on grafting degree and MFI value (DCP 0.5 wt.%, MAH 6.0 wt.%)

Effect of DCP content on the grafting degree and MFI

At a DAP/MAH molar ratio of 0.5 and MAH content of 4.0 wt.%, the effect of DCP content on the grafting degree of MAH and MFI value is shown in Fig. 3. With increasing DCP concentration, the grafting degree first increases and then decreases. The highest grafting degree of MAH is obtained when DCP content is 0.5 wt.%. The MFI value of grafted PP for the same series increases sharply when the amount of DCP is higher than 0.5 wt.%, which means that a severe degradation of the PP backbone is induced. This suggests that an appropriate amount of DCP is effective in improving the grafting degree of MAH. However, when DCP content is excessive, the grafting degree of MAH decreases because of severe chain scission of PP. Similar results have been obtained by other researchers [28, 40, 41].

Effect of MAH content on the grafting degree and MFI

At a DAP/MAH molar ratio of 0.5 and DCP content of 0.5 wt.%, the effect of MAH content on the grafting degree and MFI value is given in Fig. 4. As MAH concentration increases, the grafting degree of MAH also first increases and then decreases. As MAH content increases, more MAH monomer can react with the PP macroradicals, so the grafting degree increases. With further increase in MAH content, DAP content also increases. It suggests that MAH and DAP are involved in competitive reactions, such as grafting or cross-linking (xylene-insolubles were found in the grafted PP), which leads to a lower grafting degree and MFI value. When the DAP/MAH molar ratio is 0.5, DCP and MAH contents are 0.5 and 6.0 wt.%, respectively, the grafting degree is 1.3 wt.%.

Table 1 DSC data for pure PP, PP-g-MAH and PP-g-MAH/DAP

Sample	T_c (°C)	T_m (°C)	ΔH_c (J/g)	ΔH_m (J/g)
PP	117.0	166.9	86.7	−85.3
PP-g-MAH	118.2	165.2	83.2	−82.1
PP-g-MAH/DAP	121.8	166.4	82.6	−81.7

Effect of DAP/MAH molar ratio on the grafting degree and MFI

Figure 5 shows the grafting degree and MFI curves as a function of DAP/MAH molar ratio, obtained at MAH content of 6.0 wt.% and DCP content of 0.5 wt.%. The introduction of DAP improves the grafting degree. At a DAP/MAH molar ratio of 0.3, the grafting degree reaches a maximum of 1.5 wt.%, which is an enhancement of 88 % compared with the pure MAH system (0.8 wt.%). A furan derivative was used as co-agent in MAH grafted PP to control degradation due to its higher reactivity towards PP macroradicals with respect to MAH [32]. Similarly, TMPTA-assisted MAH grafting onto PP achieved high MAH grafting degree, attributing to high reactivity of TMPTA to PP macroradicals and MAH [36]. In the present work, the high reactivity of DAP is activated by the initiator at high temperature [42], which means that DAP can react with macroradicals to form stabilized radicals to reduce chain scission and promote the grafting process. However, the grafting degree decreases above a DAP/MAH molar ratio of 0.3. Insoluble gels form during the purification of PP-g-MAH/DAP by xylene refluxing when the DAP/MAH molar ratio is above 0.3, which hints more DAP may be involved in competitive reactions, including grafting and cross-linking. The MFI of the grafted PP therefore decreases with increasing DAP concentration. Sengupta et al. [37] also found that the influence of chain scission on melt grafting

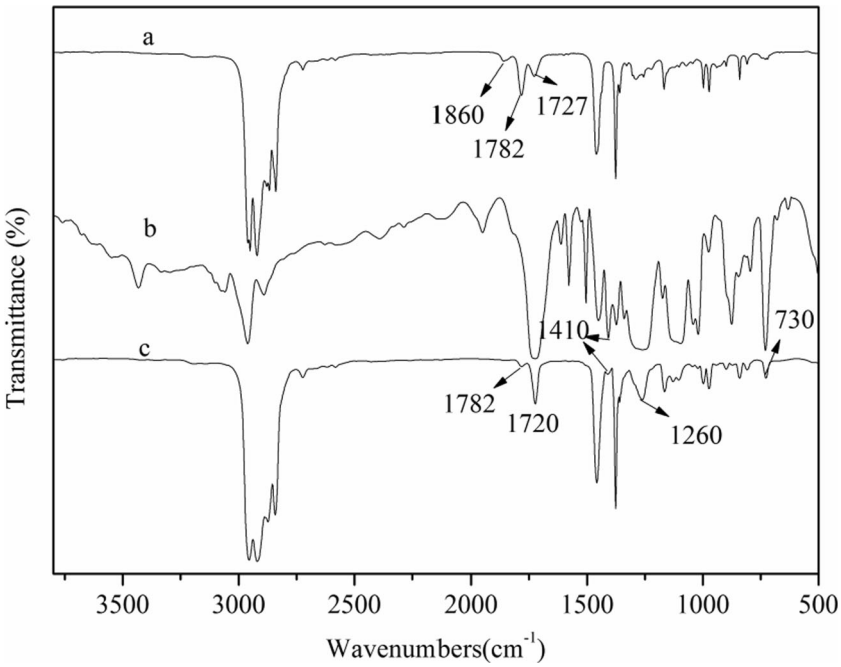

Fig. 6 FTIR spectra of (**a**) PP-g-MAH/DAP, (**b**) rPET and (**c**) PP/rPET/(PP-g-MAH/DAP) (80/20/10) blend after extracting the rPET phase

could be mitigated using TAP assisted cross-linking. A further advantage of adopting DAP is that its polar ester group can provide additional polarity as the target of grafted PP [36].

Thermal properties of grafted PP

The crystallization and melting behavior of pure PP, PP-g-MAH (G_{MAH}=0.8 wt.%) and PP-g-MAH/DAP (G_{MAH}= 1.5 wt.%) were characterized by DSC to determine the crystallization temperature (T_c), melting temperature (T_m), crystallization enthalpy (ΔH_c) and melting enthalpy (ΔH_m), as summarized in Table 1.

The T_c of grafted PP shifts to higher temperature, which implies that the nucleation capacity is enhanced, ascribed to the nucleating capability of the grafted groups. Similar results have also been reported by other authors [18, 43]. Grafted PP has a lower T_m than that of pure PP because grafting partially destroys the ordered structure of the PP crystals [30, 37, 44]. Chain scission of PP during grafting may also contribute to the decrease in T_m [30, 44]. Besides, the T_m of PP-g-MAH/DAP is higher than that of PP-g-MAH. This may be explained by the benzene ring and ester group in DAP restricting the movement of PP chain. In addition, a decrease of the melting and crystallization enthalpies is observed for grafted PP, which implies a lower crystallinity due to the presence of the grafted groups. Similar effects have been observed by other researchers [18, 30].

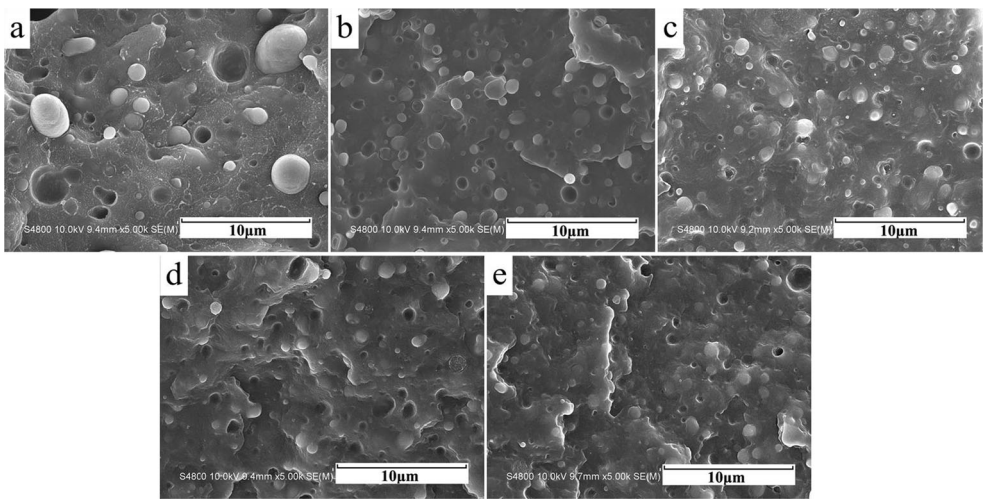

Fig. 7 SEM images of the PP/rPET/(PP-g-MAH/DAP) blends with composition (**a**) 80/20/0, (**b**) 80/20/2, (**c**) 80/20/5, (**d**) 80/20/10, (**e**) 80/20/15

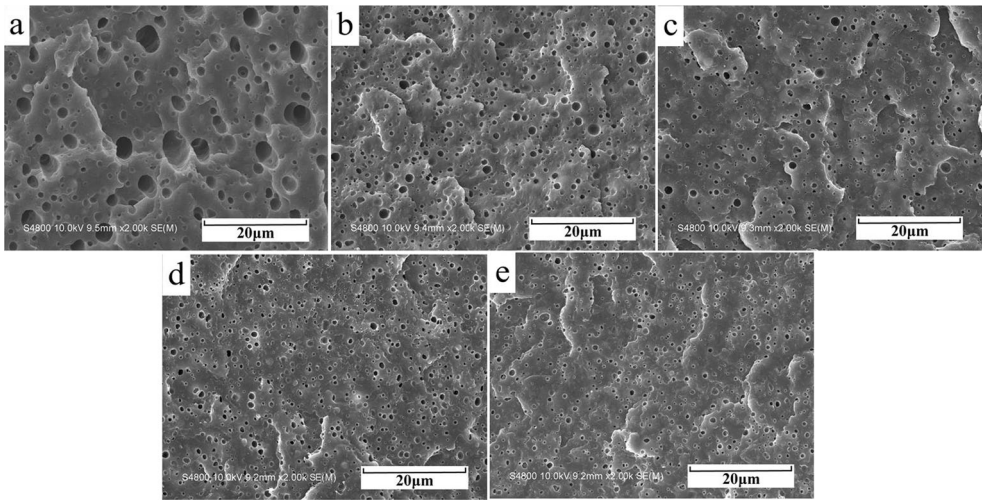

Fig. 8 SEM images of the PP/rPET/(PP-g-MAH/DAP) blends after etching the rPET phase with composition (**a**) 80/20/0, (**b**) 80/20/2, (**c**) 80/20/5, (**d**) 80/20/10, (**e**) 80/20/15

Chemical reaction between PP-g-MAH/DAP and rPET

FTIR spectra of PP-g-MAH/DAP, rPET and PP/rPET/(PP-g-MAH/DAP) (80/20/10) blend after extracting the rPET phase are given in Fig. 6. The absorption bands at 1720 cm^{-1}, 1410 cm^{-1}, 1260 cm^{-1} and 730 cm^{-1} in rPET are assigned to the stretching vibration of C=O, the benzene ring skeleton, C-O and the out-of-plane bending vibration of C=O on the benzene ring, respectively, and these bands are still found in PP/rPET/(PP-g-MAH/DAP) (80/20/10) blend after extracting the rPET phase (the band at 1727 cm^{-1} for PP-g-MAH/DAP may

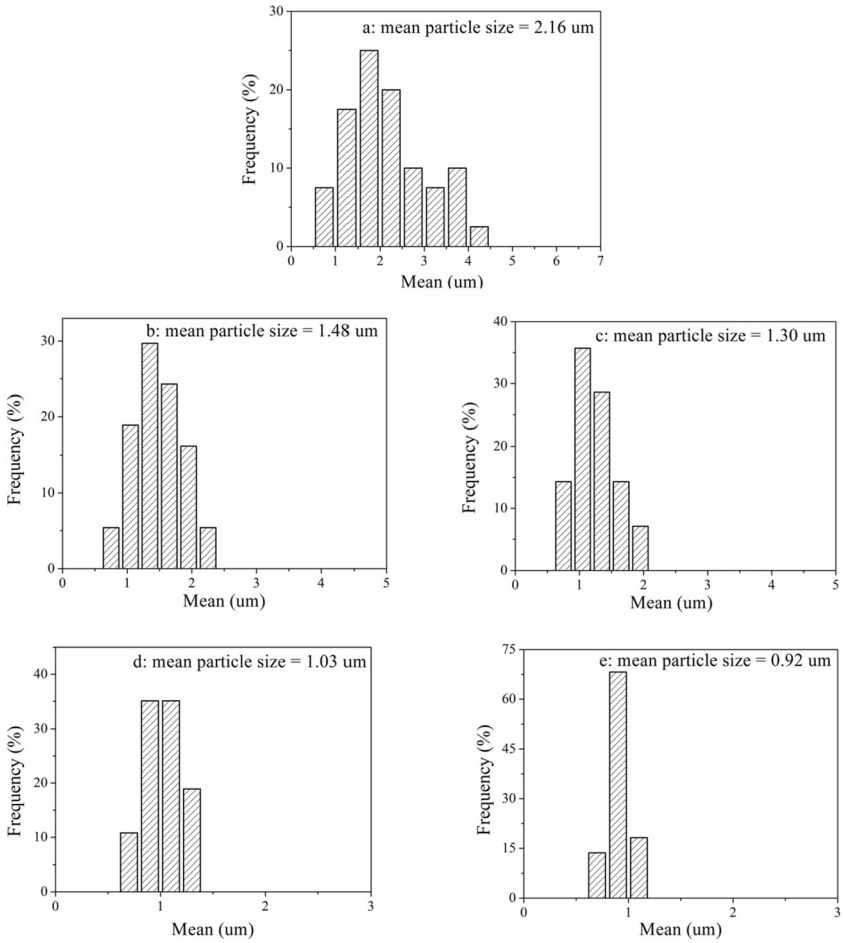

Fig. 9 Particle size distribution histograms of the PP/rPET/(PP-g-MAH/DAP) blends after etching the rPET phase with composition (**a**) 80/20/0, (**b**) 80/20/2, (**c**) 80/20/5, (**d**) 80/20/10, (**e**) 80/20/15

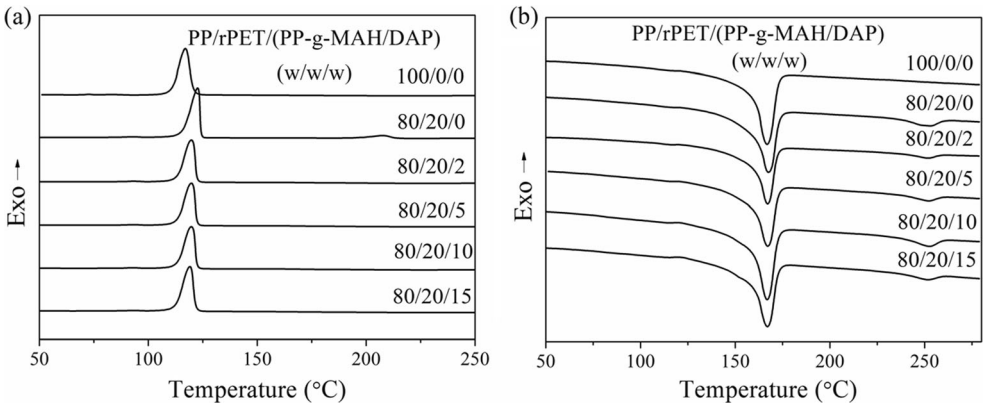

Fig. 10 DSC crystallization (**a**) and melting (**b**) curves of pure PP, PP/rPET, and PP/rPET/(PP-g-MAH/DAP) blends

be hidden by the band at 1720 cm^{-1} in the blend). The existence of the characteristic peaks of rPET in the blend after extracting the rPET phase indicates that a copolymer PP-g-PET has been in-situ generated during melting blending process owing to the chemical reaction between PP-g-MAH/DAP and the terminal groups of rPET [4].

Morphology

Figure 7 shows SEM micrographs of the uncompatibilized and compatibilized PP/rPET (80/20) blends and Figs. 8 and9 display SEM images and particle size distribution histograms of these blends with different PP-g-MAH/DAP contents after etching the dispersed rPET phase, respectively.

In Figs. 7 and 8, without a compatibilizer, the PP/rPET blend shows a dispersed rPET phase with irregular particle sizes and shapes, caused by thermodynamical immiscibility of PP and rPET. Poor interfacial adhesion is evidenced by the lack of adhered rPET on the surface of PP phase.

Figure 9, the average particle sizes of PP/rPET blends with 0, 2, 5, 10, and 15 wt.% PP-g-MAH/DAP are estimated to be 2.16, 1.48, 1.30, 1.03, and 0.92 um, respectively, and a more uniform particle size distribution of the dispersed rPET phase with increasing PP-g-MAH/DAP content is observed. It suggests that the rPET particle sizes depend on the amount of compatibilizer and that the interfacial adhesion is promoted significantly by its incorporation.

It is well known that a compatibilizer can prevent coalescence and reduce the interfacial tension in the control of morphology of a blend [21, 26, 45]. The uniformity of particle size and the shape of the rPET phase caused by adding a compatibilizer is believed to be the result of reduction of coalescence due to steric stabilization by a compatibilizer. The change of rPET particle sizes with different amounts of compatibilizer is probably caused by the different extents of interaction between the anhydride groups of MAH and the hydroxyl groups or carboxyl groups of rPET [2, 4, 17, 22]. Moreover, in this case, PP-g-MAH/DAP has similar chemical properties to the rPET phase due to the presence of the ester polar group of DAP in grafted PP, which may further enhance the interaction between PP-g-MAH/DAP and rPET, decreasing the interfacial tension at the PP-rPET interface.

Thermal properties of the blends

The effects of PP-g-MAH/DAP on the crystallization and melting behaviours of PP/rPET blends were investigated. DSC curves are given in Fig. 10 and DSC results for PP, rPET, and PP/rPET/(PP-g-MAH/DAP) blends are summarized in Table 2.

The T_c and ΔH_c of PP in the uncompatibilized PP/rPET blend are higher than those of pure PP, indicating the heterogeneous nucleating effect of rPET matrix on the continuous PP domain [4, 18]. In addition, the T_c of rPET in the uncompatibilized blend also moves to a higher temperature, which means that the PP phase also affects the nucleation of the rPET phase. Tao [4] found similar results in PP/rPET blends.

As PP-g-MAH/DAP content increases, the T_c of PP decreases, which is attributed to the interaction between PP-g-MAH/DAP and rPET [4]. The ΔH_c values of PP in the compatibilized blends are hardly affected by the PP-g-MAH/DAP content. However, a crystallization peak of rPET is not found in the compatibilized blends, which is also ascribed to the interaction between PP-g-MAH/DAP and rPET. Other researchers also reported that the crystallization of PET in the PET/PP blend was hindered by addition of SEBS-g-MAH [20]. The T_m and ΔH_m of PP and rPET show no obvious change after compatibilization, and are minimally influenced by the PP-g-MAH/DAP content.

Possible shifts in the T_g of the PP and rPET phases were studied by DMA. The T_g values of the PP and rPET phases in different blends, determined from the peaks of tan δ curves, are shown in Fig. 11. The T_g values of the PP phase hardly change, and only small peaks are observed in these locations, but the tan δ peaks for the rPET phase are influenced significantly by addition of different compatibilizer contents. The

Table 2 DSC results for PP, rPET, and PP/rPET/(PP-g-MAH/DAP) blends

PP/rPET/(PP-g-MAH/DAP)	PP				rPET			
	T_c (°C)	T_m (°C)	ΔH_c (J/g)[a]	ΔH_m (J/g)	T_c (°C)	T_m (°C)	ΔH_c (J/g)	ΔH_m (J/g)
100/0/0	116.9	167.0	69.4	−68.2	/	/	/	/
80/20/0	122.7	167.5	75.7	−72.3	207.4	252.4	6.9	−5.1
80/20/2	120.2	167.1	75.6	−72.9	/	252.3	/	−4.5
80/20/5	119.8	167.1	75.2	−73.2	/	252.0	/	−4.7
80/20/10	119.5	166.9	74.9	−71.6	/	251.9	/	−4.5
80/20/15	119.1	167.0	75.4	−72.6	/	251.8	/	−4.4
0/100/0	/	/	/	/	192.3	252.2	7.3	−7.9

[a] ΔH_c and ΔH_m were normalized by PP or rPET content

addition of 15 wt.% PP-g-MAH/DAP to the PP/rPET blend shifts the tan δ peak by 3.2 °C towards that of pure PP (9.0 °C). This is an indication of enhanced compatibility between PP and rPET phases induced by PP-g-MAH/DAP, which is supported by the morphology characterization and the DSC analysis. Heino et al. [23] also found a similar tan δ peak shift in the PP/PET/SEBS-g-MAH (80/20/5) blend.

Mechanical properties

The effects of PP-g-MAH/DAP on the tensile, flexural, and impact properties of PP/rPET blends are given in Fig. 12. As shown in Fig. 12a, blending the PP and rPET components without a compatibilizer causes a very low elongation at break because of the absence of interface adhesion. In comparison with uncompatibilized PP/rPET blend, the tensile properties of PP/rPET/(PP-g-MAH/DAP) blends show definite improvement because the compatibilizer can enhance the compatibility between two components [20, 22]. The tensile strength and elongation at break of the ternary blends first gradually increase with the increased PP-g-MAH/DAP content. Increasing PP-g-MAH/DAP content to 5 wt.%, the tensile strength and elongation at break reach maximum values of 37.5 MPa and 242 %, which are improved by 12 and 171 %, respectively, compared with the binary PP/rPET blend. However, exceeding the optimum amount of the compatibilizer, the tensile properties start to decrease slightly. This behavior may be attributed to the low tensile property of PP-g-MAH/DAP itself. When compared with pure PP (33.0 MPa), the tensile strengths of the ternary PP/rPET/(PP-g-MAH/DAP) blends improve to different degrees (the largest improvement is 14 %), whereas the elongations at break decrease due to higher tensile strength of rPET and low elongation at break of PP-g-MAH/DAP and rPET [17].

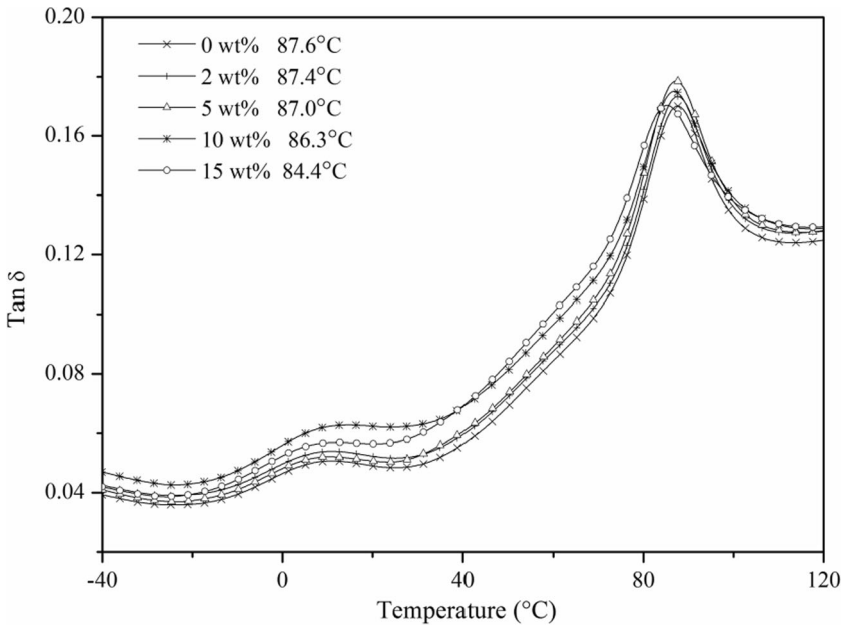

Fig. 11 Tan δ curves of the PP/rPET blends with different amounts of PP-g-MAH/DAP

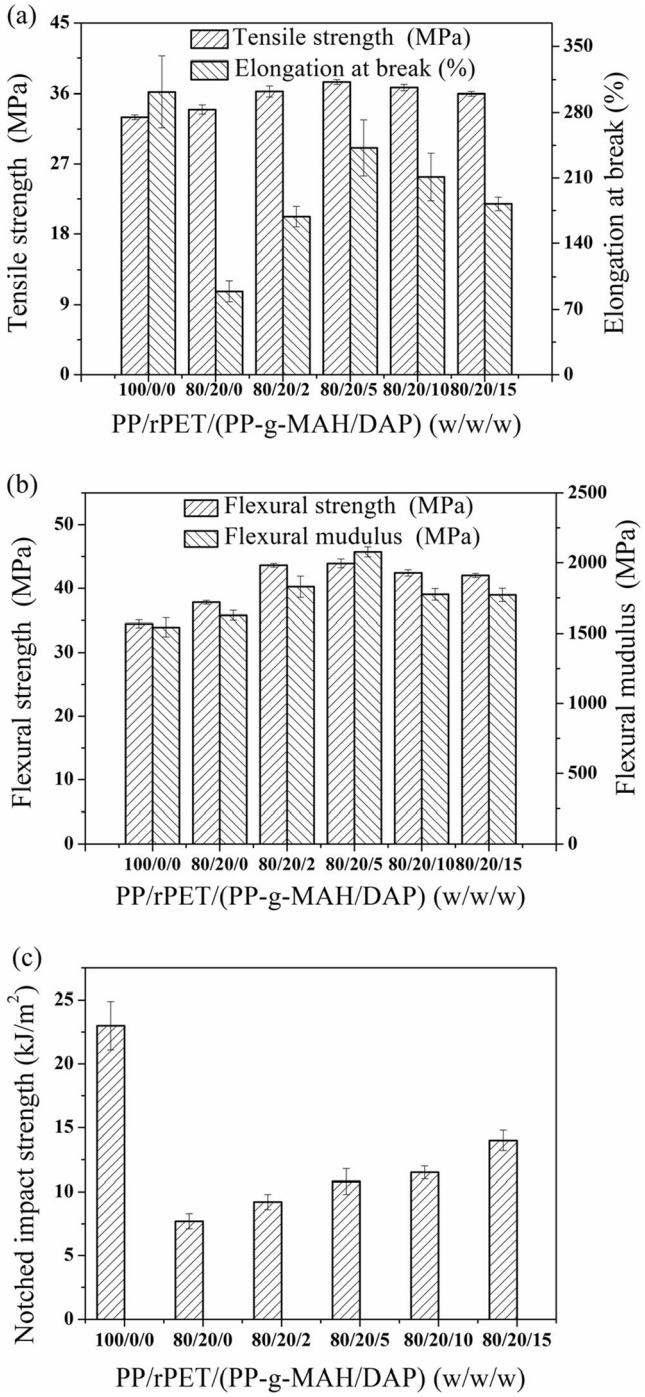

Fig. 12 Mechanical properties of pure PP, PP/rPET, and PP/rPET/(PP-g-MAH/DAP) blends. (a) Tensile property, (b) flexural property, (c) notched impact strength

The flexural properties of PP/rPET/(PP-g-MAH/DAP) show a similar trend to the tensile properties as previously mentioned, compared with the binary PP/rPET blend. Fig. 12b illustrates that variation in the PP-g-MAH/DAP content in the blends results in an increase in flexural strength and flexural modulus, followed by a slight reduction at concentrations above 5 wt.%. The flexural properties of PP/rPET blends with and without a compatibilizer are higher than those of pure PP because of the high flexural property of rPET. When the PP-g-MAH/DAP content is 5 wt.%, the value of flexural strength and flexural modulus are 43.9 MPa and 2078 MPa, which are improved by 27 and 35 %, respectively, compared with pure PP.

The notched impact strengths of the ternary PP/rPET blends are higher than that of the binary blend, as seen in Fig. 12c. When the PP-g-MAH/DAP content is 15 wt.%, the value of the notched impact strength is 14.0 kJ/m^2, improved by 82 % in comparison with the binary PP/rPET blend. This is because that the dispersed rPET particles in the ternary blends, uniformly distributed in the PP domain, are much smaller than those in the binary blend, therefore, can absorb much impact energy [46]. The notched impact strength increases with increasing PP-g-MAH/DAP content, which is supported by the morphology characterization, DSC and DMA analysis. However, the notched impact strengths of the binary and ternary blends are lower than that of pure PP, which may be related to the low notched impact strength of rPET and PP-g-MAH/DAP.

Conclusions

In this study, DAP is chosen as a co-agent for MAH grafted PP. With addition of a suitable amount of the co-agent, the grafting degree of MAH is significantly enhanced and the MFI simultaneously reduced, which means the degree of chain scission can be depressed. When the DCP and MAH contents are 0.5 and 6.0 wt.%, respectively, and the DAP/MAH molar ratio is 0.3, a maximum grafting degree of MAH (1.5 wt.%) is obtained. Meanwhile, the T_c of PP-g-MAH/DAP is higher than that of pure PP, due to the nucleating capability of the grafted groups.

The chemical reactions that take place between PP-g-MAH/DAP and rPET cause a noticeable improvement of adhesion at the PP-rPET interface, with better phase dispersion. In the binary PP/rPET blend, the T_c values of PP and rPET phases increase ascribed to the heterogeneous nucleation effect on each other. In the compatibilized PP/rPET blends, the decrease in the T_c of PP phase compared with the uncompatibilized PP/rPET blend, the disappearance of the crystallization peak of rPET phase, and the shifts in the T_g of the rPET phase towards that of PP phase are the further indications of improved adhesion at the PP-rPET interface induced by PP-g-MAH/DAP. Furthermore, the incorporation of PP-g-MAH/DAP in PP/rPET blends improves the mechanical properties with respect to the uncompatibilized PP/rPET blend.

Acknowledgments We gratefully acknowledge the Fundamental Research Funds for the Central University and the financial support of Jiangsu Hanneng Electric Co., Ltd.

References

1. Taepaiboon P, Junkasem J, Dangtungee R, Amornsakchai T, Supaphol P (2006) In situ microfibrillar-reinforced composites of isotactic polypropylene/recycled poly (ethylene terephthalate) system and effect of compatibilizer. J Appl Polym Sci 102(2):1173–1181
2. Pracella M, Rolla L, Chionna D, Galeski A (2002) Compatibilization and properties of poly (ethylene terephthalate)/polyethylene blends based on recycled materials. Macromol Chem Phys 203(10–11): 1473–1485
3. Oromiehie A, Mamizadeh A (2004) Recycling PET beverage bottles and improving properties. Polym Int 53(6):728–732
4. Tao Y, Mai K (2007) Non-isothermal crystallization and melting behavior of compatibilized polypropylene/recycled poly (ethylene terephthalate) blends. Eur Polym J 43(8):3538–3549
5. Tao Y, Pan Y, Zhang Z, Mai K (2008) Non-isothermal crystallization, melting behavior and polymorphism of polypropylene in β-nucleated polypropylene/recycled poly (ethylene terephthalate) blends. Eur Polym J 44(4):1165–1174
6. Lin Z, Shen J, Chen C, Zhang X (2011) Polypropylene/wasted poly (ethylene terephthalate) fabric composites compatibilized by two different methods: crystallization and melting behavior, crystallization morphology, and kinetics. J Appl Polym Sci 121(4):1972–1981
7. Bettini SH, de Mello LC, Munoz PA, Ruvolo Filho A (2013) Grafting of maleic anhydride onto polypropylene, in the presence and absence of styrene, for compatibilization of poly (ethylene terephthalate)/(ethylene–propylene) blends. J Appl Polym Sci 127(2): 1001–1009
8. Friedrich K, Evstatiev M, Fakirov S, Evstatiev O, Ishii M, Harrass M (2005) Microfibrillar reinforced composites from PET/PP blends: processing, morphology and mechanical properties. Compos Sci Technol 65(1):107–116
9. Oyman Z, Tincer T (2003) Melt blending of poly (ethylene terephthalate) with polypropylene in the presence of silane coupling agent. J Appl Polym Sci 89(4):1039–1048
10. Sombatdee S, Amornsakchai T, Saikrasun S (2012) Reinforcing performance of recycled PET microfibrils in comparison with liquid crystalline polymer for polypropylene based composite fibers. J Polym Res 19(3):1–13
11. Atta A, Abdel-Rauf M, Maysour N, Abdul-Rahiem AM, Abdel-Azim A-A (2006) Surfactants from recycled poly (ethylene terephthalate) waste as water based Oil spill dispersants. J Polym Res 13(1):39–52
12. Saikrasun S, Limpisawasdi P, Amornsakchai T (2009) Comparative study on phase and properties between rPET/PS and LCP/PS in situ microfibrillar-reinforced composites. J Polym Res 16(4):443–454
13. Liu S, Zhou L, Li L, Yu S, Liu F, Xie C, Song Z (2013) Isooctanol alcoholysis of waste polyethylene terephthalate in acidic ionic liquid. J Polym Res 20(12):1–6
14. Asgari M, Masoomi M (2012) Thermal and impact study of PP/PET fibre composites compatibilized with glycidyl methacrylate and maleic anhydride. Compos Part B: Eng 43(3):1164–1170
15. Si X, Guo L, Wang Y, K-t L (2008) Preparation and study of polypropylene/polyethylene terephthalate composite fibres. Compos Sci Technol 68(14):2943–2947
16. Jayanarayanan K, Thomas S, Joseph K (2008) Morphology, static and dynamic mechanical properties of in situ microfibrillar composites based on polypropylene/poly (ethylene terephthalate) blends. Compos Part A: Appl Sci 39(2):164–175
17. Chiu H-T, Hsiao Y-K (2006) Compatibilization of poly (ethylene terephthalate)/polypropylene blends with maleic anhydride grafted polyethylene-octene elastomer. J Polym Res 13(2):153–160
18. Pracella M, Chionna D (2003) Reactive compatibilization of blends of PET and PP modified by GMA grafting. Macromol Symp 198(1): 161–172
19. Bae TY, Park KY, Kim DH, Suh KD (2001) Poly (ethylene terephthalate)/polypropylene reactive blends through isocyanate functional group. J Appl Polym Sci 81(5):1056–1062
20. Papadopoulou C, Kalfoglou N (2000) Comparison of compatibilizer effectiveness for PET/PP blends: their mechanical, thermal and morphology characterization. Polymer 41(7):2543–2555
21. Pang Y, Jia D, Hu H, Hourston D, Song M (2000) Effects of a compatibilizing agent on the morphology, interface and mechanical behaviour of polypropylene/poly (ethylene terephthalate) blends. Polymer 41(1):357–365
22. Yoon KH, Lee HW, Park OO (1998) Properties of poly(ethylene terephthalate) and maleic anhydride-grafted polypropylene blends by reactive processing. J Appl Polym Sci 70(2):389–395
23. Heino M, Kirjava J, Hietaoja P (1997) Compatibilization of polyethylene terephthalate/polypropylene blends with styrene–ethylene/butylene–styrene (SEBS) block copolymers. J Appl Polym Sci 65(2): 241–249
24. Calcagno CI, Mariani CM, Teixeira SR, Mauler RS (2009) Morphology and crystallization behavior of the PP/PET nanocomposites. J Appl Polym Sci 111(1):29–36
25. Shi W, Li Y, Xu J, Ma G, Sheng J (2007) Morphology development in multi-component polymer blends: I composition effect on phase morphology in PP/PET polymer blends. J Macromol Sci Part B: Phys 46(6):1115–1126
26. Akbari M, Zadhoush A, Haghighat M (2007) PET/PP blending by using PP-g-MA synthesized by solid phase. J Appl Polym Sci 104(6): 3986–3993
27. Saujanya C, Radhakrishnan S (2001) Structure development and properties of PET fibre filled PP composites. Polymer 42(10): 4537–4548
28. Li Y, Xie XM, Guo BH (2001) Study on styrene-assisted melt free-radical grafting of maleic anhydride onto polypropylene. Polymer 42(8):3419–3425
29. Bettini S, Ruvolo Filho A (2008) Styrene-assisted grafting of maleic anhydride onto polypropylene by reactive processing. J Appl Polym Sci 107(3):1430–1438
30. Henry GR, Drooghaag X, Rousseaux DD, Sclavons M, Devaux J, Marchand Brynaert J, Carlier V (2008) A practical way of grafting maleic anhydride onto polypropylene providing high anhydride contents without sacrificing excessive molar mass. J Polym Sci, Part A: Polym Chem 46(9):2936–2947
31. Drooghaag X, Rousseaux DDJ, Henry GRP, Sclavons M, Carlier V, Marchand-Brynaert J (2010) Mediated melt functionalization of polypropylene. Polym Degrad Stab 95(3):342–345
32. Augier S, Coiai S, Gragnoli T, Passaglia E, Pradel JL, Flat JJ (2006) Coagent assisted polypropylene radical functionalization: monomer grafting modulation and molecular weight conservation. Polymer 47(15):5243–5252
33. Coiai S, Passaglia E, Aglietto M, Ciardelli F (2004) Control of degradation reactions during radical functionalization of polypropylene in the melt. Macromolecules 37(22):8414–8423
34. Coiai S, Augier S, Pinzino C, Passaglia E (2010) Control of degradation of polypropylene during its radical functionalisation with furan and thiophene derivatives. Polym Degrad Stab 95(3):298–305
35. Zhu L, Tang G, Shi Q, Cai C, Yin J (2006) Neodymium oxide-assisted melt free-radical grafting of maleic anhydride on isotactic-

polypropylene by reactive extrusion. J Polym Sci, Part B: Polym Phys 44(1):134–142
36. Ni QL, Fan JQ, Niu H, Dong JY (2011) Enhancement of graft yield and control of degradation during polypropylene maleation in the presence of polyfunctional monomer. J Appl Polym Sci 121(5): 2512–2517
37. Sengupta SS, Parent JS, Chaudhary BI (2009) Selectivity of allylic coagent-mediated polypropylene maleation. Polym Eng Sci 49(10): 1945–1950
38. Jayanarayanan K, Bhagawan SS, Thomas S, Joseph K (2007) Morphology development and non isothermal crystallization behaviour of drawn blends and microfibrillar composites from PP and PET. Polym Bull 60(4):525–532
39. De Roover B, Sclavons M, Carlier V, Devaux J, Legras R, Momtaz A (1995) Molecular characterization of maleic anhydride-functionalized polypropylene. J Polym Sci, Part A: Polym Chem 33(5):829–842
40. Lei C, Li S, Chen D, Wu B, Huang W (2011) Melt grafting of maleic anhydride onto polypropylene with 1-decene as a second monomer. J Appl Polym Sci 119(1):102–110
41. Shi D, Hu GH, Li R (2006) Concept of nano-reactor for the control of the selectivity of the free radical grafting of maleic anhydride onto polypropylene in the melt. Chem Eng Sci 61(11):3780–3784
42. Simpson W, Holt T, Zetie R (1953) The structure of branched polymers of diallyl phthalate. J Polym Sci 10(5):489–498
43. Seo Y, Kim J, Kim KU, Kim YC (2000) Study of the crystallization behaviors of polypropylene and maleic anhydride grafted polypropylene. Polymer 41(7):2639–2646
44. Luo W, Liu X, Fu Y (2012) Melt grafting of maleic anhydride onto polypropylene with assistance of α-methylstyrene. Polym Eng Sci 52(4):814–819
45. Lepers JC, Favis BD, Tabar RJ (1997) The relative role of coalescence and interfacial tension in controlling dispersed phase size reduction during the compatibilization of polyethylene terephthalate/polypropylene blends. J Polym Sci, Part B: Polym Phys 35(14):2271–2280
46. Cui YY, Dong BJ, Li BL, Li SC (2013) Properties of polypropylene/poly(ethylene terephthalate) thermostimulative shape memory blends reactively compatibilized by maleic anhydride grafted polyethylene-octene elastomer. Int J Polym Mater 62(13):671–677